International Journal of Innovative Computing, Information and Control
Volume **20**, Number **6**, December **2024**

 ISSN 1349-4198
pp. **1621–1634**

DESIGN OF A SILICON PHOTONIC 3-DB THREE-MODE POWER SPLITTER

Duy Nguyen[1], Thuy Tran[2], Nghia Thi Mai[2], Kotaro Hashikura[3]
Md Abdus Samad Kamal[3], Iwanori Murakami[3], Dung Cao Truong[2]
Hung Tan Nguyen[4] and Kou Yamada[3]

[1]Graduate School of Science and Technology
[3]Division of Mechanical Science and Technology
Gunma University
1-5-1 Tenjincho, Kiryu, Gunma 376-8515, Japan
{ t232b604; k-hashikura; maskamal; murakami; yamada }@gunma-u.ac.jp

[2]Faculty of Electronics Engineering 1
Posts and Telecommunications Institute of Technology
122 Hoang Quoc Viet, Cau Giay District, Hanoi 11355, Vietnam
{ thuyttt; nghiamt; dungtc }@ptit.edu.vn

[4]The Advanced Institute of Science and Technology
The University of Danang
41 Le Duan, Hai Chau, Da Nang 50001, Vietnam
hung.nguyen@ac.udn.vn

Received February 2024; revised May 2024

Abstract. *Silicon photonics has emerged as a crucial technology, driven by advancements in optical communications, particularly for data center communication transceivers. The rapid growth in silicon photonics is fueled by breakthroughs and increased investment. Leveraging the unique properties of silicon, such as high refractive index contrast and compatibility with Complementary Metal-Oxide-Semiconductor (CMOS), a variety of passive and active photonic devices have been developed, facilitating high-bandwidth data transmission. Building upon the capabilities of silicon photonics, this paper proposes a design for a 3-dB power splitter capable of accommodating three modes simultaneously. The proposed structure is designed on a Silicon-on-Insulator (SOI) material platform with a silicon layer thickness of 220 nm, following the standards of VLSI chip fabrication technology. The entire geometric structure is optimized, and its optical performance is evaluated using the 3D-BPM numerical simulation method. Simulation results demonstrate that the proposed structure operates effectively over a wide spectral range of 70 nm (from 1520 nm to 1590 nm). The overall integrated footprint of the structure is compact. These advantages in optical performance hold promise for the integration of large-scale photonic circuits, as well as in wideband Mode Division Multiplexing (MDM) technology applications.*

Keywords: 3-dB power splitter, Mode division multiplexing, Silicon photonics, Three-mode simultaneously, Trident-coupler

1. **Introduction.** Recently, with the robust growing demand of ultra-high bandwidth in optical communication networks, a variety of multiplexing techniques have been utilized in order to enhance the traffic throughput. Mode Division Multiplexing (MDM) technique has been regarded as a promising solution, along with Wavelength Division Multiplexing (WDM), to increase bandwidth capacity [1, 2]. This technique, besides some emerging techniques such as Nyquist superchannel [3], and single sideband modulation [4], has been

DOI: 10.24507/ijicic.20.06.1621

considered an attractive method to surpass Shannon's information theory limits [5], especially, in short-reach optical transmission systems when the multimode dispersion problem is inconsiderable in a short distance. MDM can further boost transmission capacity by deploying communication channels in high-order modes [6]. Recently, MDM within Few-Mode Fiber (FMF) has been extensively investigated as a promising approach to enhance data capacity while allowing for controlled mode manipulation [7, 8]. However, handling the issues of mode division multiplexing channels as well as mode conversion in an optical fiber can present significant challenges and require a cumbersome mechanism for implementation. As a result, techniques for mode conversion and mode division multiplexing by manipulating optical waveguides using silicon-on-insulator technology can offer numerous substantial benefits, including high flexibility, compactness, low loss, and reasonable cost. These advantages stem from the excellent characteristics of the silicon photonic platform, which features a high refractive index contrast resulting in low bending loss and a small spot-size mode distribution. Moreover, silicon photonics exhibits low propagation loss within the telecom windows due to minimal wavelength spectrum absorption. Additionally, silicon photonics, when implemented using a standard Silicon-on-Insulator (SOI) wafer, is compatible with the CMOS manufacturing process for very large-scale integrated electronic circuits, enabling mass production capabilities [9].

Currently, there is a strong demand for a coupler that can bridge the gap between Few-Mode Fiber (FMF) and silicon integrated chips. Nevertheless, achieving efficient FMF-chip coupling with minimal mode crosstalk remains a significant challenge, primarily due to the substantial spot-size difference between few-mode fiber modes and waveguide modes. Fortunately, coupling between a fiber mode and a waveguide mode in the fundamental mode can be easily achieved via Bragg diffraction gratings. Consequently, the task of converting high-order fiber modes is simplified to high-order waveguide mode conversion, a task easily accomplished using silicon waveguides [10, 11].

Optical power splitters play a crucial role in Photonic Integrated Circuits (PICs), serving various applications such as phased arrays, power monitoring, and lattice filters [12]. The ability to customize power splitting ratios is essential for these applications. Directional Couplers (DCs) offer flexibility in achieving desired ratios but are sensitive to wavelength and have strict fabrication tolerances [13]. Multimode Interference (MMI) couplers, despite having higher losses, are attractive due to their broad bandwidth and forgiving fabrication tolerances [14]. Achieving customizable ratios in MMIs typically involves specialized geometries like the butterfly structure [15] and bent design [16], which introduce variable input/output port spacing and angles, making integration challenging. Alternatively, cascaded MMIs with phase-control sections [17] and MMIs with computer-generated planar holograms offer fixed port spacing and angles but demand precise fabrication for phase control and holograms [18].

Many papers have shown their attention to the design of a 3-dB power split on the silicon-on-insulator platform. In [19], they introduced ultra-compact polarization-independent 3-dB power splitter for fundamental mode with size of 1.2 μm × 2.62 μm with an operating bandwidth from 1540 to 1590 nm. Authors in [20] reported on a compact 2×2 3-dB adiabatic coupler designed using the shortest mode transformer method for TE_0 mode. By optimizing the profile of the waveguide widths and the gap spacing, the compact 3-dB coupler was designed with a short coupling length of 23.2 μm. The fabricated device exhibits a 3-dB splitting ratio with less than ±0.3 dB power oscillation and a low excess loss of 0.23 dB over a broad wavelength range of 1485-1620 nm. In [21], an ultracompact broadband dual-mode 3-dB power splitter using inverse design method for highly integrated on-chip mode (de)multiplexing system was proposed and experimentally demonstrated. A dual-mode convertor based on subwavelength axisymmetric three-branch

waveguide is utilized to convert TE_0 and TE_1 to three intermediate fundamental modes. The axisymmetric topology constraint of the nanostructures enables the optimized device to achieve a strict 3-dB splitting ratio over a broad wavelength range from 1.52 to 1.60 μm. In [22], they proposed a silicon-based power splitter based on a Subwavelength Grating (SWG)-assisted Multimode Interference (MMI) structure for TE_0 mode. In [23], the design of a silicon photonic broadband Y-splitter for fundamental mode by particle-swarm optimization algorithm was presented. Their device operated in the broad wavelength range 1250 nm-1550 nm. In [24], researchers proposed and demonstrated on-chip power splitters based on adiabatic rib waveguides, enabling arbitrary splitting ratios on a monolithic silicon photonic platform. These devices feature engineered adiabatic directional couplers with trapezoid structures in the longitudinal mode evolution region. Measurement results show that the proposed devices achieve over 150 nm bandwidth for splitting ratios of 50% : 50%, 70% : 30%, and 90% : 10%, with a mode evolution footprint narrowed to below 79 μm and an insertion loss of less than 0.22 dB. [25] introduced a design for a 3-dB power splitter based on SOI technology. The design features three cuboidal waveguides with rectangular cross-sectional areas. A power of 10 mW is injected into the primary waveguide port, which is then evenly split between the secondary waveguides, resulting in a 3-dB power split at the output ports. Approximately 45% of the total power is transferred to each of the secondary waveguides, ensuring balanced power distribution. In all the above manuscripts, the proposed devices for 3-dB splitter use only one fundamental mode. Therefore, in this study we propose a 3-dB splitter capable of accommodating three modes simultaneously, including fundamental mode TE_0, first-order mode TE_1 and second-order mode TE_2.

In this paper, we propose a novel structure for a 3-dB power splitter capable of handling multiple modes. This structure combines a self-image 2×2 MMI coupler, Y-junction, and trident-coupler. The proposed device is based on Silicon-on-Insulator (SOI) technology and operates in the C-band, centered at 1550 nm. We utilize 3D-BPM simulations for optimization to evaluate the effectiveness of device. This device is essential for achieving the full functionality of on-chip optical networks using Mode Division Multiplexing (MDM) technology. The main contributions of this work are as follows:

1) Application of the phase matching condition in trident-coupler to using multimode;
2) Proposal of 3-dB three-mode power splitter based on silicon photonic waveguides, which makes high performance for the potential applications of high-speed communication integrated systems;
3) Optimizing the geometric structure of the power splitter and evaluating its optical performance using the rigorous 3D-Beam Propagation Method (3D-BPM) numerical simulations.

The remaining part of the paper is organized as follows. Section 2 describes the proposed device's structure and principle. Section 3 demonstrates and analyzes the device characterization. Finally, Section 4 summarizes the research.

2. **Design and Structural Optimization.**

2.1. **Optimization method.**

The optimization method employed in this study aims to enhance the performance of the proposed silicon photonic devices. By systematically adjusting various parameters, such as geometric dimensions, the algorithm iteratively refines the design to achieve predefined objectives, such as maximizing transmission efficiency. This optimization process leverages numerical simulations and mathematical algorithms to efficiently explore the design space and identify optimal configurations, thereby facilitating the development of high-performance photonic devices.

2.1.1. *3D-BPM.* The 3D-BPM (Three-Dimensional-Beam Propagation Method) is a computational technique used to analyze the propagation of optical waves through complex three-dimensional photonic structures. By numerically solving the Maxwell's equations, this method simulates the behavior of light as it travels through waveguides, splitters, and other photonic components. 3D-BPM enables accurate predictions of optical properties such as transmission spectra, mode profiles, and scattering characteristics, allowing researchers to optimize device designs and evaluate performance metrics before fabrication. This method plays a crucial role in the design and optimization of advanced photonic devices for various applications, including telecommunications, sensing, and computing.

2.1.2. *EIM.* The Effective Index Method (EIM) is a computational technique utilized in the design and optimization of photonic devices. This method simplifies the analysis of wave propagation in photonic structures by approximating the effective refractive index of the modes supported by the structure.

2.2. **General description.** The proposed 3-dB power splitter device is illustrated in Figure 1 from a top-down view.

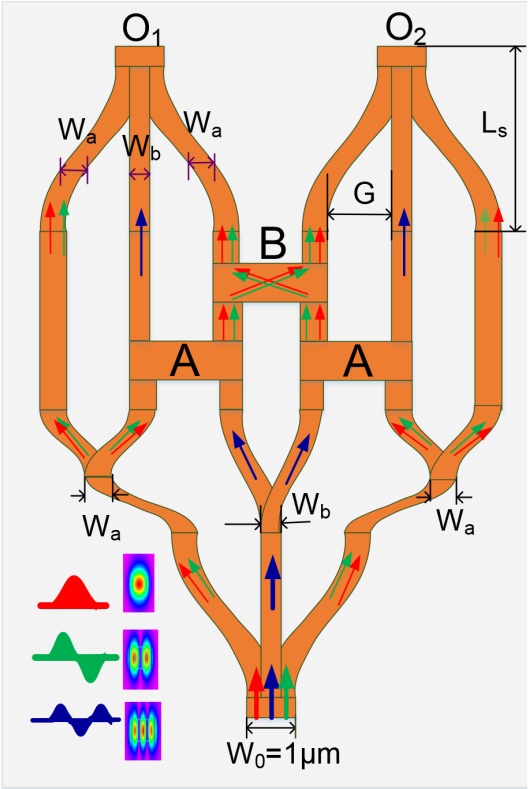

FIGURE 1. (color online) The design diagram of the proposed 3-dB power splitter

The waveguide structure comprises several bends and straight segments, forming a complex path for the signal to split and combine before reaching the output ports. It includes three Multimode Interference (MMI) couplers and three trident-couplers. The splitter has two output ports, O_1 and O_2, with the input port located at the bottom center, having a width of $W_0 = 1$ µm. The waveguide segments are divided into two types with different widths: W_a and W_b. The trident-coupler's vertical length is denoted as L_s, and the distance G represents the gap of the trident-coupler. Labels A (length $L_{MMI\text{-}A}$ and width $W_{MMI\text{-}A}$) and B (length $L_{MMI\text{-}B}$ and width $W_{MMI\text{-}B}$) identify specific regions known as MMI couplers, where particular interactions and splitting of the signal occur. The

field distributions at various points are depicted with red (representing the fundamental mode TE_0), green (representing first-order mode TE_1), and blue (representing second-order mode TE_2) waveforms, along with corresponding color-coded intensity profiles. Red, green, and blue arrows indicate the direction of power flow within the waveguides.

The structure diagram of the division (de)multiplexing device according to three modes with output is two branches according to $1+1$ protection circuit mode. The total length of the device is 660 μm. The waveguide structure is symmetrically configured in a $1:2$ arrangement, i.e., one input and two outputs. It consists of a trident-coupler in the form of a Ψ-junction coupler as the input waveguide branch, with a multimode waveguide base supporting three-mode Transverse Electric (TE) polarization, specifically TE_0, TE_1, and TE_2. The designed structure incorporates three identical Ψ-shaped junction mechanisms, one serving as the input and the other two for the two output branches. Within the structure, three Y-junctions are employed for branching, and three couplers are used according to the self-image 2×2 MMI coupler. The parameters of the device structure are presented in Table 1.

TABLE 1. The parameters of the proposed device

Parameter	Dimension (μm)	Parameter	Dimension (μm)
W_a	0.5	$L_{MMI\text{-}A}$	37
W_b	0.4	$L_{MMI\text{-}B}$	39
W_0	1	L_s	120
G	1.25	h_{SiO2}	0.7
$W_{MMI\text{-}A}$	1.7	$W_{MMI\text{-}B}$	2.05

The conceptual diagram of the 1×2 3-dB mode power splitter is used to split power between output in ports O_1 and O_2. The operating principles of the 3 modes are shown by the arrows in Figure 1. The fundamental mode and TE_1 have the same operating principle. When injecting these two modes into the waveguide, their power is evenly divided between the two arms of the trident-coupler, while TE_2 mode converts into TE_0 and propagates straight to the middle waveguide. Next, at Y-junction, fundamental mode is split equally for both branches.

Our proposed device is based on SOI channel waveguides with 220 nm-thick top on insulator wafer illustrated in Figure 2. The operation wavelength $\lambda = 1550$ nm and the refractive indices of the silicon core layer and the cladding silica layer are $n_r = 3.465$ and $n_c = 1.445$, respectively. The proposed device is fabricated by using modern methods; for instance, the whole device is fabricated by using E-beam lithography method and dry etching technique as Inductively Coupled Plasma (ICP) etching technique in the form of the channel waveguides from a standard 220 nm-slab height.

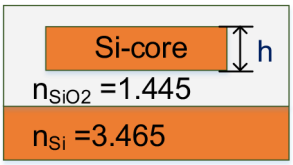

FIGURE 2. The size view of the proposed schematic

2.3. **Trident-coupler.** The design of the trident-coupler includes a main waveguide with a width of W_0 and 3 bus wave guides, including 2 S-bent waveguides with a width of W_a and a straight waveguide with a width of W_b. Following the phase matching conditions

principle described in [26], this trident-coupler is designed to guide two modes, TE_0 and TE_1, along two branches on both sides, while mode TE_2 is converted into TE_0 and follows the central waveguide. The device is designed to support the operation of three-mode in the three-dimension mechanism in the Transverse Electric (TE) modes polarizations states at the central wavelength of 1550 nm. EIM method is used to find out the effective index coefficients of guided three-mode in the main waveguide W_0. The simulation tool with mode solver by nonvectorial 3D-BPM method is utilized to observe the quantity of guided modes. It can be seen that in Figure 3 the effective index depends on width of the waveguide. As a result, W_0 can be chosen from 0.75 μm to 1.05 μm to support three-mode transmission. In the design, we choose $W_0 = 1$ μm. And then this waveguide is coupled with three waveguides, the middle is the straight waveguide with the width of $W_b = 0.4$ μm and the length is $L_s = 120$ μm, two waveguide symmetrical 2-side in sinusoidal form (S-bent waveguide) has a width of $W_a = 0.5$ μm with a length and a gap of L_s and $G = 1.25$ μm, respectively.

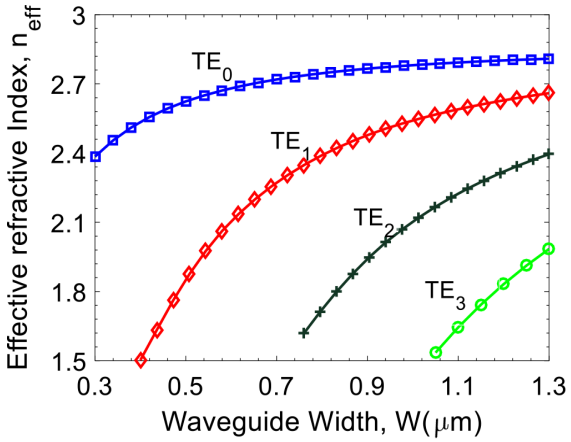

FIGURE 3. Simulation effective indices for different modes of the trident-coupler as a function of stem input width using BPM method

2.4. **2 × 2 MMI coupler.**

2.4.1. *Principle of* 2 × 2 *MMI coupler.* The functioning principle of the suggested 2 × 2 MMI coupler adheres to the Talbot's effect [27]. In the underlying interference mechanism [14], the passage of signals through the MMI is subject to alterations contingent on both the length of MMI and the placement of the waveguide via the MMI. Specifically, the self-image of a 2 × 2 MMI coupler has a length of $L_{MMI} = 3L_\pi$ [28]. This length, denoted as L_π for the MMI coupler, can be determined using the following relationship:

$$L_\pi = \frac{4n_{eff}W_e^2}{3\lambda}, \tag{1}$$

where

$$W_e = W_{MMI} + \frac{\lambda}{\pi}\left(n_{eff}^2 - n_c^2\right)^{-0.5}. \tag{2}$$

Here, W_e is effective width of MMI region for TE mode, λ is operation wavelength, n_{eff} is effective index, and n_c is refractive index of the cladding layer. Besides, we use 3D-BPM simulation to optimize the length of L_{MMI} to get the desired self-image when passing each MMI respectively. We found the optimal MMI length and the best transmission to be $L_{MMI\text{-}A} = 37$ μm and $L_{MMI\text{-}B} = 39$ μm, based on Figure 4.

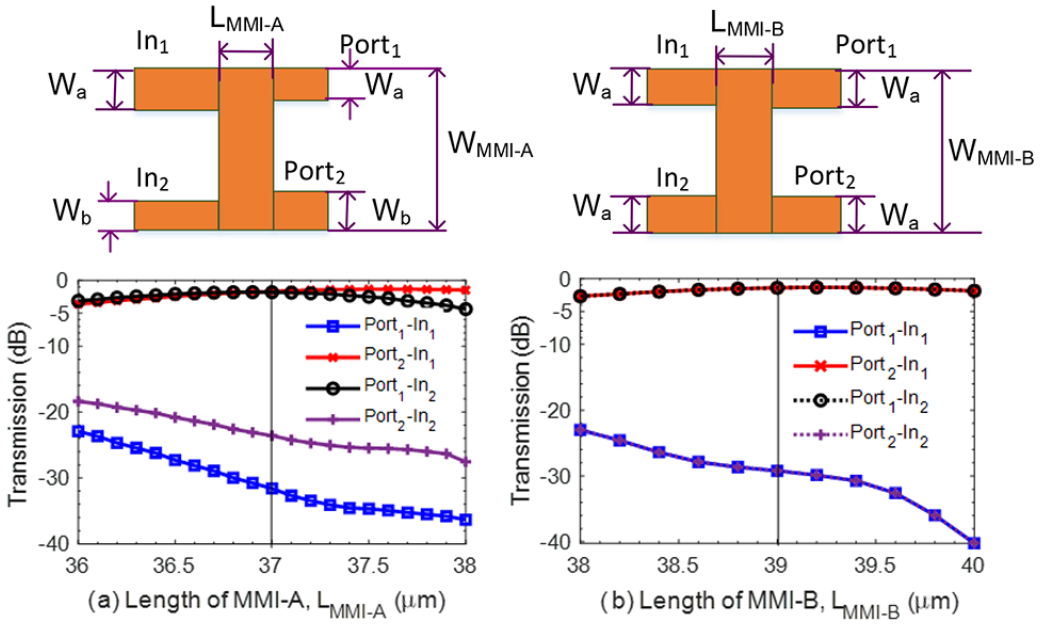

FIGURE 4. Optimizing the MMI using 3D-BPM numerical simulation: (a) For MMI-A; (b) for MMI-B

2.4.2. *Sensitivity analysis of* 2×2 *MMI coupler.* The multimode interferences including MMI-A and MMI-B couplers presented in Figure 4 exhibit a dependency of transmission characteristics on the lengths $L_{MMI\text{-}A}$ and $L_{MMI\text{-}B}$.

The structure of MMI-A is characterized by the input port widths W_a and W_b and the output port widths W_a and W_b, respectively. The transmission characteristics shown in Panel (a) indicate a significant sensitivity of the transmission to variations in $L_{MMI\text{-}A}$.

The length $L_{MMI\text{-}A}$ significantly influences the light interference within the MMI region. As $L_{MMI\text{-}A}$ varies, the transmission at the output ports shows notable differences. Specifically, the asymmetrical design, with $W_a > W_b$, results in different transmission characteristics for Port_1 and Port_2 when inputs In_1 and In_2 are injected. In contrast, $L_{MMI\text{-}B}$ shows much less sensitivity to length variations. Due to the symmetrical design of MMI-B, where the input and output port widths are equal, the transmission characteristics at Port_1 and Port_2 are nearly identical. This symmetry ensures that the light interference is uniformly distributed.

The sensitivity analysis reveals that $L_{MMI\text{-}A}$ is more affected by length variations due to the asymmetrical port widths, causing significant differences in transmission between Port_1 and Port_2. The insertion loss efficiency deteriorates with length deviations, necessitating a fabrication tolerance of ± 0.5 μm to maintain optimal performance. In contrast, the symmetrical design of $L_{MMI\text{-}B}$ ensures stable and identical transmission characteristics at both output ports, making it less sensitive to length variations and allowing for a more relaxed fabrication tolerance of ± 1 μm. This insight is crucial for optimizing the design and fabrication of MMI couplers in photonic integrated circuits.

2.5. **Symmetric Y-junction.** Symmetric Y-junctions, also known as Y-couplers or 3-dB couplers, are essential components in optical systems and integrated photonics. In our research, these Y-junctions serve the purpose of power splitting.

3. **Simulation Results and Discussion.** In this section, we present the simulation results and provide a discussion.

3.1. **Trident-coupler.** Figure 5 presents the transmission characteristics and wavelength -dependent spectra of the Ψ-coupler, simulated numerically. Panel (a) depicts the structure of the trident-coupler with three ports: Port_1, Port_2, and Port_3. Phase matching plays a crucial role in the performance of the trident-coupler. For the TE_0 mode, the input signal is equally split into the two branches, efficiently directing the power to Port_1 and Port_3. For the TE_1 mode, the input signal transforms into the TE_0 mode in the two branches, ensuring efficient power transfer to Port_1 and Port_3 with even less coupling to Port_2. Panels (b) and (c) show the transmission spectra for the fundamental TE_0 and first-order TE_1 modes across a wavelength range of 1.52 to 1.59 μm. The results show a transmission efficiency of about −4 dB at Port_1 and Port_3 for both modes. Port_2 experiences crosstalk, with levels ≤ -28 dB for the TE_0 mode and ≤ -40 dB for the TE_1 mode. In contrast, the TE_2 mode, shown in panel (d), primarily converts into the TE_0 mode in the central branch, resulting in a transmission efficiency around −3 dB at Port_2 and ≤ -20 dB at Port_1 and Port_3. The trident-coupler shows robust performance across a range of wavelengths, making it suitable for broadband applications in integrated photonic circuits.

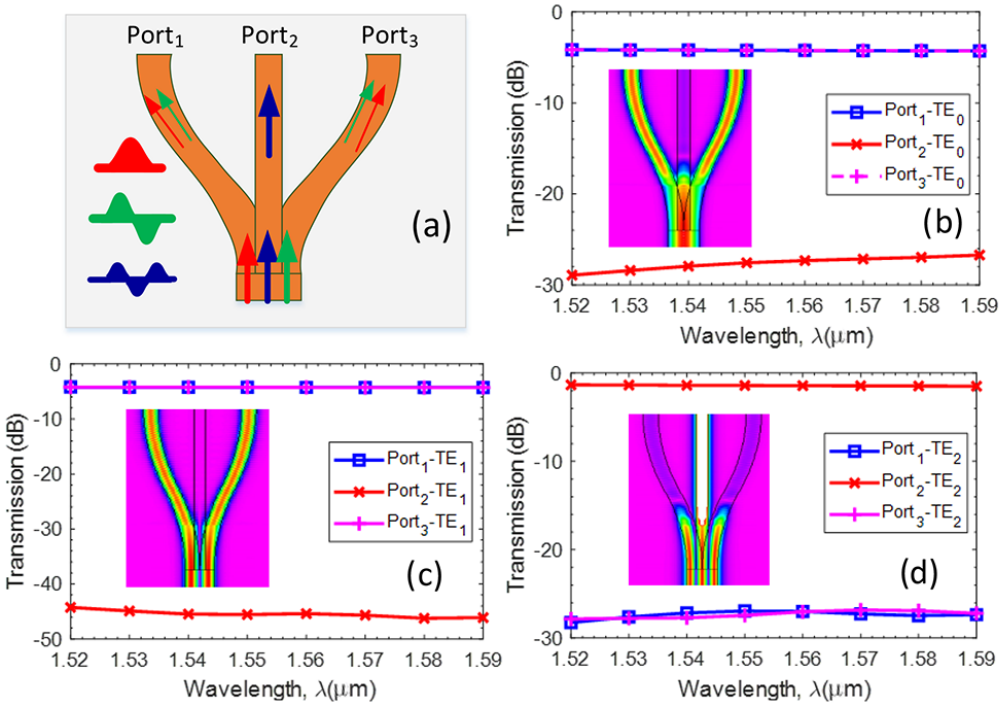

FIGURE 5. The transmission characteristics and wavelength-dependent spectra for the Ψ-coupler are simulated numerically. (a) Structure of the trident-coupler, (b) TE_0 mode, (c) TE_1 mode and (d) TE_2 mode.

3.2. **2×2 MMI coupler.** The simulation results presented in Figures 6(a1), (a2), (a3), (b1), (b2), (b3) illustrate the performance comparison between two Multimode Interferometers (MMIs), denoted as MMI-A and MMI-B, across varying wavelengths. Panels (a1) and (a2) show the field distribution for MMI-A with inputs at In_1 and In_2, respectively, while panels (b1) and (b2) depict the corresponding field distributions for MMI-B. The transmission spectra, depicted in Panels (a3) and (b3), reveal the wavelength-dependent transmission characteristics of the ports for MMI-A and MMI-B configurations, respectively.

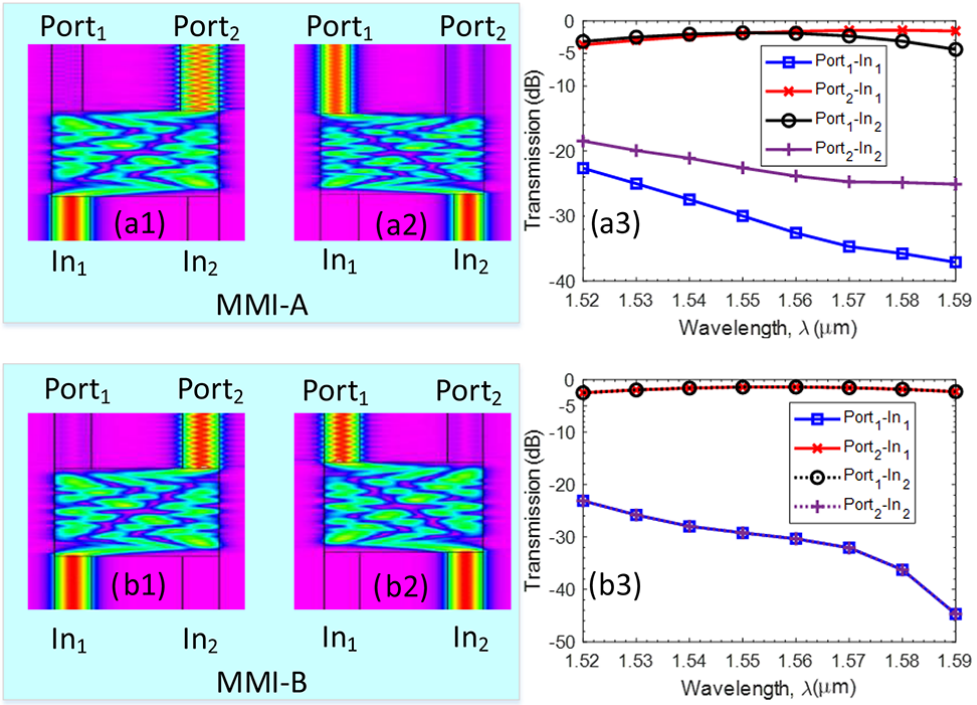

FIGURE 6. Simulated electromagnetic field distributions and the wavelength spectra of power outputs for the 2×2 MMI couplers: (a1), (a2) and (a3) for MMI-A; (b1), (b2) and (b3) for MMI-B

3.3. **The device.** Figure 7 illustrates the results obtained from the BPM simulation, showing the electric field distribution for the TE_0, TE_1, and TE_2 modes of the device at an operating wavelength of 1550 nm. The results show compatibility with the above device performance analysis, and a small fraction the emission is negligible from the core to the clad. The figures (a), (b), and (c) represent the field patterns for the TE_0, TE_1, and TE_2 modes, respectively, with a 50 : 50 split ratio. The color-coded intensity profiles, ranging from 0.0 to 1.0, indicate the power distribution within the waveguide structure. The red regions represent the areas with the highest intensity, while the blue regions indicate lower intensity. In all three cases, the field distributions demonstrate that the signal is effectively guided through the waveguide structure with minimal loss. The patterns show a clear confinement of the modes within the core, with only a negligible fraction of the emission leaking into the cladding. This confirms the efficiency of the waveguide design in maintaining the integrity of the signal. The simulation results align well with the expected device performance, showcasing the effective splitting and combining capabilities of the waveguide structure for multiple modes at the designated wavelength. This demonstrates the robustness and efficiency of the proposed design in handling multimode signals.

In order to evaluate the performances of the proposed device in terms of topics, we consider parameter to be power defined as

$$P_{xy} = 10 \log_{10} \frac{P_{out}}{P_{in}}, \tag{3}$$

where P_{xy} represents the ratio of output power to input with $x = 1, 2$ denoting the output port and $y = 0, 1, 2$ representing the mode TE_0, TE_1 and TE_2. P_{in} is the normalized input power, and P_{out} is the optical power at the corresponding output port.

Figure 8 demonstrates the transmission characteristics spectra of power monitored by 3D-BPM over the wavelength range from 1520 nm to 1590 nm of the C-band. At different

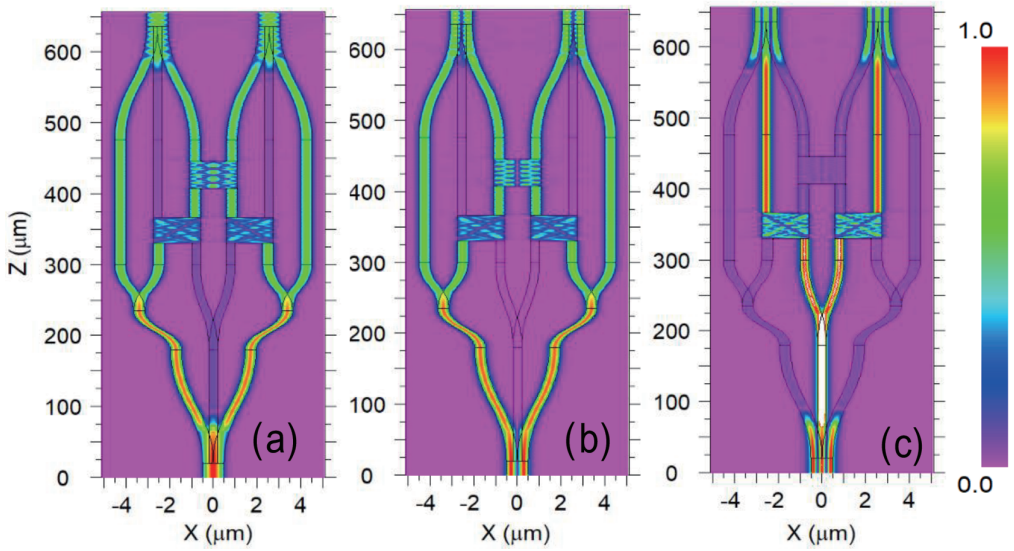

FIGURE 7. (color online) Simulated electric field patterns for the proposed three-mode power split with a 50 : 50 split ratio are shown in figures (a), (b), and (c) for the TE_0, TE_1, and TE_2 modes, respectively.

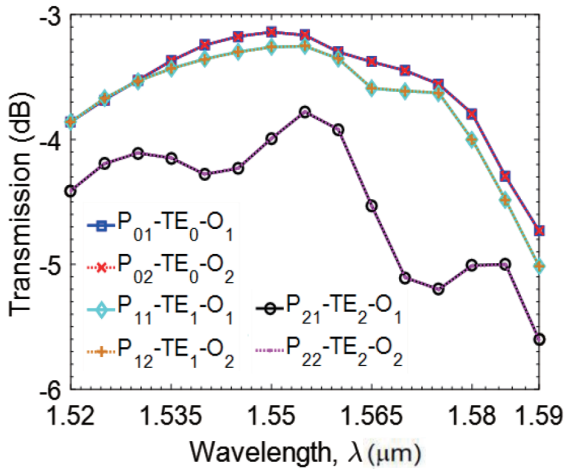

FIGURE 8. The optimal performance characteristic of the device depends on the active wavelength for the three modes.

wavelengths, the power at both output ports of the device remains 3-dB. The power ratio at the two ports for TE_0 and TE_1 modes in the wavelength range from 1.52 nm to 1.59 nm is approximately between -5 dB to -3 dB, whereas the power for mode TE_2 is lower, ranging from about -5.5 dB to -4 dB.

Therefore, our proposed device, which operates as a power splitter, exhibits consistent performance across the wavelength range studied. The maintenance of a 3-dB power split at different wavelengths indicates the device's stability and reliability in dividing the input power evenly between its output ports. This characteristic is crucial in various optical communication systems where signal integrity and balance between different channels are paramount. Furthermore, the observed power ratios for TE_0, TE_1, and TE_2 modes provide insights into the device's mode-selective behavior. The slight variations in power distribution among different modes highlight the device's capability to handle different polarization states, which is advantageous in applications requiring polarization diversity or manipulation.

In practical optical networks, such as wavelength-division multiplexing WDM and MDM systems, devices like these play a vital role in distributing optical signals efficiently and maintaining signal quality across multiple channels. The ability to split power with minimal loss and maintain consistent performance across a broad wavelength range enhances the overall efficiency and reliability of such networks, making the device a valuable component in optical communication infrastructure.

4. **Conclusion.** The paper proposes a design for a 3-dB splitting optical circuit accommodating three orthogonal waveguide modes, based on silicon photonics technology and the SOI material platform. Components built upon Ψ-junctions, sinusoidal waveguides, and multi-mode interference couplers are fundamental elements of the Silicon photonics integrated circuit. The design optimization and optical characteristic evaluations are carried out through 3D-BPM numerical simulations. The results demonstrate effective splitting and combining of the modes with minimal loss and negligible emission into the cladding. The confinement of the modes within the core across the specified wavelength range confirms the robustness of the design. Besides, the simulation results indicate that the mode-splitting structure performs well over a wavelength range of 70 nm, spanning from 1520 nm to 1590 nm. Furthermore, the compact design holds promise for potential applications in large-scale integrated photonics circuits as well as high-density mode division multiplexing signal processing systems.

Despite these promising results, this study has certain limitations. Firstly, the research is limited to a fixed 50 : 50 splitting ratio. This constraint reduces the flexibility and applicability of the design in scenarios requiring variable power distribution. Moreover, the study primarily relies on numerical simulations without experimental validation.

Future research directions should address these limitations. Incorporating controllable phase shifters into the design could enable dynamic and flexible splitting ratios, such as 70 : 30, 10 : 90, and 40 : 60, thereby enhancing the versatility of the optical circuit. Additionally, experimental validation of the proposed design is crucial to confirm its performance and reliability. Further investigation into fabrication tolerances, temperature stability, and integration with other photonic components will also be essential for advancing the practical implementation of this technology in integrated photonics and mode division multiplexing systems.

REFERENCES

[1] Y. Tan, H. Wu and D. Dai, Silicon-based hybrid (de)multiplexer for wavelength-/polarization-division-multiplexing, *Journal of Lightwave Technology*, vol.36, no.11, pp.2051-2058, 2018.

[2] C. R. Doerr and T. F. Taunay, Silicon photonics core-, wavelength-, and polarization-diversity receiver, *IEEE Photonics Technology Letters*, vol.23, no.9, pp.597-599, 2011.

[3] M. R. M. Arnob, S. Nahar and M. N. Uddin, An empirical analysis of 5.76 Tbits/s SDM-PDM-Nyquist superchannel WDM hybrid multiplexing technique for channel capacity enhancement, *Proc. of the 2nd International Conference on Computing Advancements*, 2022.

[4] Y. Zhang, F. Zhang and S. Pan, Optical single sideband modulation with tunable optical carrier-to-sideband ratio, *IEEE Photonics Technology Letters*, vol.26, no.7, pp.653-655, 2014.

[5] R.-J. Essiambre et al., Capacity limits of optical fiber networks, *Journal of Lightwave Technology*, vol.28, no.4, pp.662-701, 2010.

[6] C. Li, D. Liu and D. Dai, Multimode silicon photonics, *Nanophotonics*, vol.8, no.2, pp.227-247, 2018.

[7] N. Borhani et al., Learning to see through multimode fibers, *Optica*, vol.5, no.8, pp.960-966, 2018.

[8] D. J. Richardson, J. M. Fini and L. E. Nelson, Space-division multiplexing in optical fibres, *Nature Photonics*, vol.7, no.5, pp.354-362, 2013.

[9] S. Y. Siew et al., Review of silicon photonics technology and platform development, *Journal of Lightwave Technology*, vol.39, no.13, pp.4374-4389, 2021.

[10] N. Do et al., Self-controlling photonic-on-chip networks with deep reinforcement learning, *Scientific Reports*, vol.11, no.1, 23151, 2021.
[11] D. D. Quang et al., 1×3 reconfigurable and simultaneous three-mode selective router based on silicon waveguide utilizing Ti microheaters as thermo-optic phase shifters, *Microelectronics Journal*, vol.117, 105278, 2021.
[12] J.-Y. Sie et al., Robust arbitrary ratio power splitter by fast quasi-adiabatic elimination in optical waveguides, *Optics Express*, vol.27, no.26, pp.37622-37633, 2019.
[13] D. Dai, J. Wang and Y. Shi, Silicon mode (de)multiplexer enabling high capacity photonic networks-on-chip with a single-wavelength-carrier light, *Optics Letters*, vol.38, no.9, pp.1422-1424, 2013.
[14] M. Bachmann, P. A. Besse and H. Melchior, Overlapping-image multimode interference couplers with a reduced number of self-images for uniform and nonuniform power splitting, *Applied Optics*, vol.34, no.30, pp.6898-6910, 1995.
[15] P. A. Besse et al., New 2/spl times/2 and 1/spl times/3 multimode interference couplers with free selection of power splitting ratios, *Journal of Lightwave Technology*, vol.14, no.10, pp.2286-2293, 1996.
[16] D. S. Levy et al., A multimode interference-based variable power splitter in GaAs-AlGaAs, *IEEE Photonics Technology Letters*, vol.9, no.10, pp.1373-1375, 1997.
[17] D. H. Ta et al., 1×2 switchable dual-mode optical 90 hybrid device based on thermo-optic phase shifters and 2×2 MMI couplers on SOI platform, *IEEE Photonics Journal*, vol.13, no.1, pp.1-16, 2021.
[18] S.-Y. Tseng, S. Choi and B. Kippelen, Variable-ratio power splitters using computer-generated planar holograms on multimode interference couplers, *Optics Letters*, vol.34, no.4, pp.512-514, 2009.
[19] A. Zhang et al., Ultra-compact polarization-independent 3dB power splitter in silicon, *Optics Letters*, vol.46, no.19, pp.5000-5003, 2021.
[20] I. K. Kim et al., High-performance and compact silicon photonic 3-dB adiabatic coupler based on shortest mode transformer method, *IEEE Photonics Journal*, vol.13, no.4, pp.1-6, 2021.
[21] W. Chang et al., Inverse design and demonstration of an ultracompact broadband dual-mode 3dB power splitter, *Optics Express*, vol.26, no.18, pp.24135-24144, 2018.
[22] Y. Shi et al., Ultra-broadband and low-loss silicon-based power splitter based on subwavelength grating-assisted multimode interference structure, *Photonics*, vol.9, no.7, MDPI, 2022.
[23] P. Maidment and M. Sorel, Ultra-broadband, low loss 3dB splitter in silicon photonics waveguides, *2022 Conference on Lasers and Electro-Optics (CLEO)*, 2022.
[24] X. Liu et al., Ultra-broadband on-chip power splitters for arbitrary ratios on silicon-on-insulator, *Optics Express*, vol.32, no.2, pp.2029-2038, 2024.
[25] D. Srivastava, S. Vardhan and R. R. Singh, SoI based optical 1×2 wavelength independent 3-dB power splitter design using three rectangular cross-sectional cuboidal waveguides, *Silicon*, vol.15, no.3, pp.1381-1391, 2023.
[26] D. N. T. Hang et al., Compact, highly efficient, and controllable simultaneous 2×2 three-mode silicon photonic switch in the continuum band, *IEEE Access*, vol.9, pp.102387-102396, 2021.
[27] P. A. Besse et al., Optical bandwidth and fabrication tolerances of multimode interference couplers, *Journal of Lightwave Technology*, vol.12, no.6, pp.1004-1009, 1994.
[28] L. B. Soldano and E. C. M. Pennings, Optical multi-mode interference devices based on self-imaging: Principles and applications, *Journal of Lightwave Technology*, vol.13, no.4, pp.615-627, 1995.

Author Biography

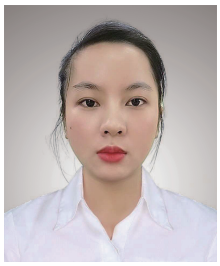

Duy Nguyen received the Engineer, and Master of Science at the Posts and Telecommunications Institute of Technology, Hanoi, in 2020, and 2023, respectively. She is currently a Ph.D. student at the Gunma University, Japan. Her research interests include photonic integrated circuits, optical communication systems, applications of AI models for big data processing and analyzing.

Thuy Tran serves as a lecturer at the Faculty of Electronics Engineering 1, Posts and Telecommunications Institute of Technology (PTIT) in Vietnam, currently. Her academic journey led her to attain a Master's degree in Telecommunication Engineering from PTIT in 2023. Presently, she is immersed in a Ph.D. program at the same institution where she imparts knowledge. Since 2018, she has been a proud member of the AI-photonics lab at PTIT. Her research focus spans areas such as photonic integrated circuits, machine learning applications in photonic networks, and optical high-speed communication systems.

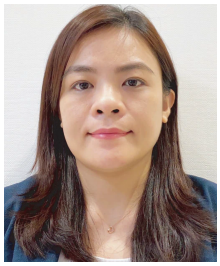

Nghia Thi Mai received the B.S., M.S. and Dr. Eng. degrees from Gunma University, Gunma, Japan in 2009, 2011 and 2014, respectively. From 2014 to 2015, she was with the Human Resources Cultivation Center, Gunma University, Gunma, Japan as a research associate. From 2015 to 2021, she worked on research on damping control for automobiles at Exedy Co., Ltd. Since 2022, she has been working as a lecturer at the Faculty of Electronics Engineering 1, Posts and Telecommunications Institute of Technology (PTIT). In addition, she is currently working as a visiting associate professor and part-time lecturer at the Department of Electronics and Mechanical Engineering, Gunma University. Her research interest includes Smith predictor, internal model control and robotics.

Kotaro Hashikura received the B.S. degree of Mechanical Engineering, the M.S. degree of Informatics, and the Dr. degree of Engineering from Kyushu Institute of Technology, Fukuoka, Japan in 2006, from Kyoto University, Kyoto, Japan in 2010, and from Tokyo Metropolitan University, Tokyo, Japan in 2014, respectively. From 2014 until 2018, he had been a project research associate at the Faculty of System Design, Tokyo Metropolitan University. He is currently an assistant professor at the Division of Mechanical Science and Technology, Gunma University, Japan. His research interests include time-delay-related control techniques, such as deadbeat, preview-prediction and repetitive controls. He is a member of IEEE, ISCIE and SICE.

Md Abdus Samad Kamal received the B.Sc. degree in Electrical and Electronic Engineering from Khulna University of Engineering and Technology (KUET), Khulna, Bangladesh in 1997, Master and Doctor degrees from Graduate School of Information Science and Electrical Engineering from Kyushu University, Japan in 2003 and 2006, respectively. He was a post-doctoral fellow in Kyushu University till November 2006. He is currently an associate professor at the Division of Mechanical Science and Technology, Gunma University, Japan. His current research interests are reinforcement learning, intelligent transportation systems, and multiagent systems. He is a member of IEEE and SICE.

Iwanori Murakami received his Ph.D. Eng. from Gunma University in 1997. He is currently an associate professor at Gunma University. His research interests include robotics, applied electromagnetics and machines, and superconducting levitation applications.

Dung Cao Truong received the Engineer, Master of Science, and Ph.D. degrees from Hanoi University of Science and Technology, Hanoi, in 2003, 2006, and 2015, respectively. He is currently an associate professor and a lecturer in Faculty of Electronics Engineering 1, Posts and Telecommunications Institute of Technology, Hanoi, Vietnam. His research interests include photonic integrated circuits, plasmonic, high-speed optical communication systems, smart IoT systems, applications of deep learning models for photonics design, and AI in photonics.

Hung Tan Nguyen received the B.E. degree from The University of Danang-University of Science and Technology, Da Nang, Vietnam, in 2003, and the M.E. and Ph.D. degrees from the University of Electro-Communications, Tokyo, Japan, in 2009 and 2012, respectively. From 2012 to 2016, he was a researcher with the National Institute of Advanced Industrial Science and Technology, Tsukuba, Japan, where he worked on ultrafast and spectrally efficient all-optical network technologies, and development of an all-optical wavelength converter. In 2016, he joined The University of Danang, Danang, Vietnam, where he is currently an associate professor and the vice-director of The University of Danang, Advanced Institute of Science and Technology. His research interests include optical communications and networking, all-optical signal processing and photonic integrated circuits.

Kou Yamada received B.S. and M.S. degrees from Yamagata University, Yamagata, Japan in 1987 and 1989, respectively, and a Dr. Eng. degree from Osaka University, Osaka, Japan in 1997. From 1991 to 2000, he was with the Department of Electrical and Information Engineering, Yamagata University, Yamagata, Japan as a research associate. From 2000 to 2008, he was an associate professor in the Department of Mechanical System Engineering, Gunma University, Gunma, Japan. Since 2008, he has been a professor in the Division of Mechanical Science and Technology, Gunma University, Gunma, Japan. His research interests include robust control, repetitive control, process control, and control theory for inverse systems and infinite-dimensional systems. Dr. Yamada received the 2005 Yokoyama Award in Science and Technology, the 2005 Electrical Engineering/Electronics, Computer, Telecommunication, and Information Technology International Conference (ECTI-CON2005) Best Paper Award, the Japanese Ergonomics Society Encouragement Award for an Academic Paper in 2007, the 2008 Electrical Engineering/Electronics, Computer, Telecommunication, Information Technology International Conference (ECTI-CON2008) Best Paper Award, and the 4th International Conference on Innovative Computing, Information and Control Best Paper Award in 2009, the 14th International Conference on Innovative Computing, Information and Control Best Paper Award in 2019, and Outstanding Achievement Award from Kanto Branch of Japanese Society for Engineering Education in 2022 and JSME (The Japan Society of Mechanical Engineers) Education Award in 2023. He is a member of IEEE and SICE, and a fellow of JSME.